Field monitoring of an unsaturated saprolitic hillslope

A.K. Leung, H.W. Sun, S.W. Millis, J.W. Pappin, C.W.W. Ng, and H.N. Wong

Abstract: To advance the understanding of the rainfall-induced landslide triggering mechanism, a comprehensive field monitoring programme was implemented in a saprolitic hillslope in Hong Kong. The instrumentation covered the measurements of the two stress-state variables (i.e., net normal stress and matric suction) and their effects. The monitoring results, including pore-water pressure (PWP), volumetric water content, subsurface total horizontal stress, horizontal displacement, and rainfall intensity, are reported. Most instruments recorded reliable and good quality data, which have strong correlation among each other. The site-specific infiltration and deformation characteristics of the hillslope subjected to heavy rainstorms are investigated. Shallow transient perched groundwater tables were believed to be developed at colluvial deposits on the top 3 m, where PWPs up to 20 kPa were typically measured. The main groundwater table probably rose by 6 m when the hillslope was subjected to rainfall intensity of 133.5 mm/h. It is possible that cross-slope groundwater flowed along a shallow, dipped decomposed rock stratum at the central portion of the landslide body. Besides, two distinct types of slope movements were generally observed, namely the "cantilever" and the "deep-seated" mode. Rupture surfaces have possibly been developed at 5 m below ground or deeper, resulting in a multiple translational- and rotational-slide type of failure.

Key words: field monitoring, instrumentation, unsaturated saprolite, earth pressure, landslide.

Résumé : Afin d'améliorer la compréhension des mécanismes de déclenchement des glissements terrains causés par les précipitations, un programme de suivi extensif sur le terrain a été implanté dans une pente saprolitique à Hong Kong. L'instrumentation comprend des mesures de deux variables de l'état des contraintes (contrainte nette et succion matricielle) et leurs effets. Les résultats du suivi incluant la pression interstitielle, la teneur en eau volumique, la contrainte totale horizontale sous la surface, le déplacement horizontal et l'intensité des précipitations sont présentés. La majorité des instruments ont enregistré des données fiables et de bonne qualité et qui comportent des fortes corrélations entre elles. L'infiltration spécifique au site à l'étude et les caractéristiques de déformation de la pente soumise à des précipitations intenses sont étudiées. Il est suggéré qu'une nappe phréatique perchée transitoire est développée dans les dépôts colluviaux sur les premiers 3 m, où des pressions interstitielles jusqu'à 20 kPa sont typiquement mesurés. La nappe phréatique principale s'élève probablement de 6 m lorsque la pente subit des précipitations d'une intensité de l'ordre de 133,5 mm/h. Il est possible qu'un écoulement d'eau souterraine à travers la pente le long d'une couche peu profonde de roche décomposée se produise dans la section centrale de la masse du glissement. Deux types de mouvements de pente sont généralement observés sur les côtés, soit le mode « en porte-à-faux » et le mode « en profondeur ». Des surfaces de rupture sont possiblement développées à 5 m sous la surface, ou plus en profondeur, ce qui entraîne un type de rupture multiple à glissement en translation et en rotation.

Mots-clés : suivi sur le terrain, instrumentation, saprolite non saturée, pression des terres, glissement de terrain.

[Traduit par la Rédaction]

Introduction

Rainfall-induced landslides are natural geological phenomena, which have caused untold numbers of catastrophic consequences in terms of casualities and economic losses worldwide. These problems are especially serious in tropical and subtropical regions such as Malaysia, Japan, Brazil, Singapore, Hong Kong, and part of the mainland China. The intrinsic geological conditions in these regions, for instance, deep weathering of rocks, likely result in deep groundwater tables, and the soils above exist frequently in unsaturated conditions. When subjected to seasonal climatic variations, the infiltration and deformation characteristics of heterogeneous unsaturated soil in the vadose zone may be complex. This may hinder the subsequent slope stability assessment. Reliable geological and hydrogeological models, which can be deduced from field inspections, ground investigation fieldworks, and field monitoring, are therefore always prerequisite information to capture the ground behaviour and to understand the landslide triggering mechanism of a hillslope subjected to severe rainfall events.

Numerous field instrumentations have been used exten-

Received 3 February 2010. Accepted 9 August 2010. Published on the NRC Research Press Web site at cgj.nrc.ca on 16 February 2011.

A.K. Leung[1] and C.W.W. Ng. Department of Civil and Environmental Engineering, Hong Kong University of Science and Technology, Clear Water Bay, Kowloon, Hong Kong.
H.W. Sun and H.N. Wong. Geotechnical Engineering Office, Civil Engineering and Development Department, Government of the Hong Kong SAR, Hong Kong.
S.W. Millis and J.W. Pappin. Arup, Hong Kong.

[1]Corresponding author (e-mail: celka@ust.hk).

Fig. 1. Overview of geomorphological setting of natural terrain and location of fieldworks. IP, instantaneous profile.

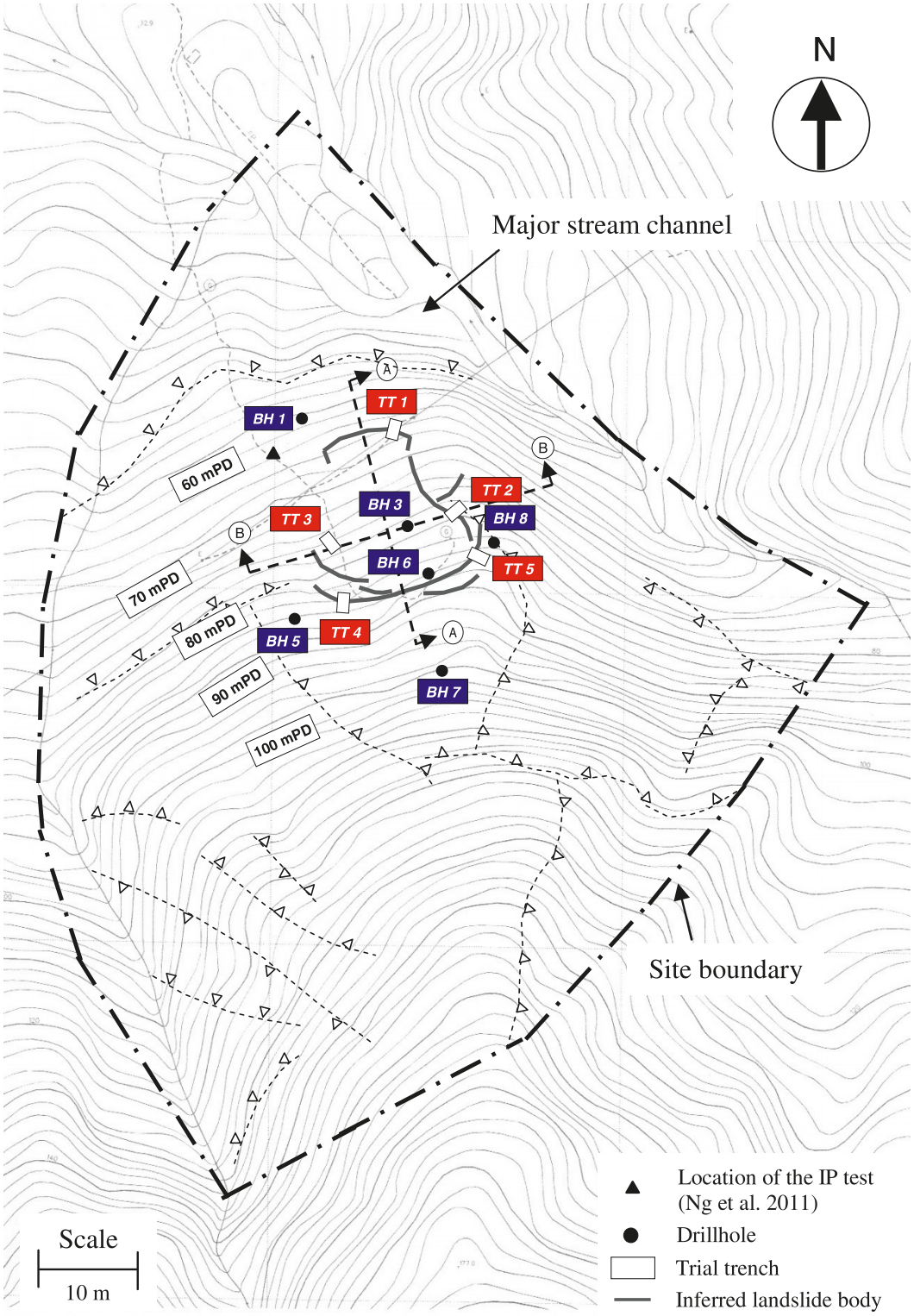

sively to investigate the infiltration characteristic and hence the response of small-scale unsaturated soil slopes under different natural or artificially applied precipitation conditions (Lim et al. 1996; Sun et al. 1998, 2000; Gasmo et al. 1999; Ng et al. 2003; Rahardjo et al. 2005; Zhan et al. 2007). Relationships among matric suction, soil moisture content, rainfall intensity, and duration were sometimes established. The matric suction was typically found to vary within the top 3 m, where transient perched water tables were frequently observed. These may be one of the major reasons causing most landslides to fail at relatively shallow regions (Bao and Ng 2000). Although unsaturated soil behaviour is recognized to be fundamentally governed by the two stress-state variables (net normal stress and matric suction; Fred-

Fig. 2. Inferred active landslide body and location of instruments. CP, Casagrande-type piezometer; EPC, earth pressure cell; IPI, in-place inclinometer; JFT, jet-filled tensiometer; SP, standpipe; TC, heat dissipation matric water potential sensor; TDR, water content reflectometer; RG, rain gauge.

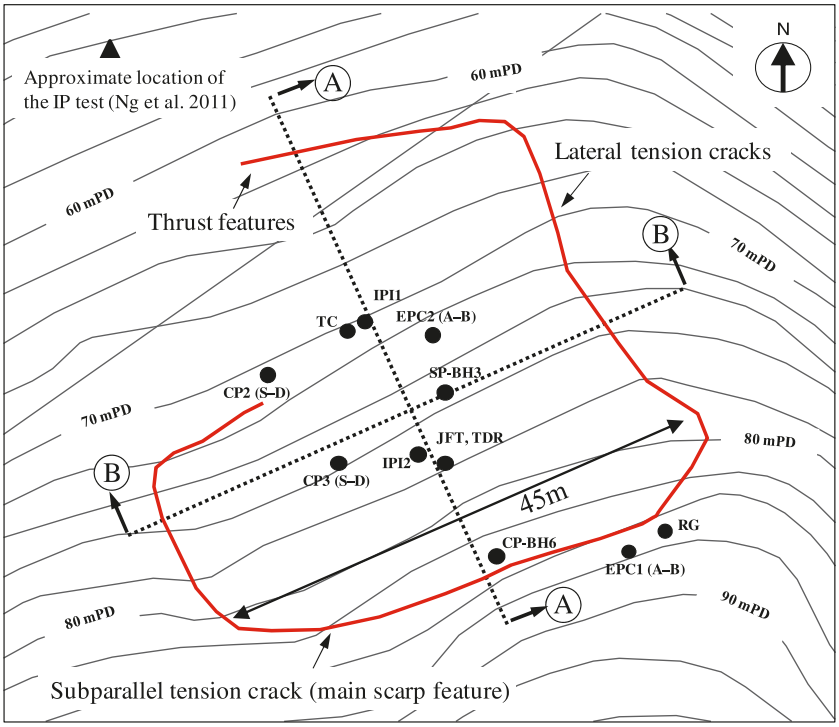

lund and Rahardjo 1993), field investigation of any effect of net normal stress on slope response is rarely studied and reported. It is obvious that the measurements of ground deformation as well as the two stress-state variables are vital to assess slope movements and landslide failure mechanisms when an advanced numerical tool such as the finite element method is used. Ng et al. (2003) described one of the very few attempts to implement a comprehensive field instrumentation scheme to investigate the influence of the two stress-state variables on the response of an unsaturated expansive soil slope. The significant increase of the total horizontal stress indicated the possibility of passive pressure failures in the softened clay upon artificially applied rainfalls.

Most of the previous field studies appeared to mainly focus on the investigation of small-scale unsaturated cut slopes based on the responses of the single stress-state variable, i.e., matric suction. When compared to a large-scale natural hillslope, the ground response may be much more difficult to capture because of the existing complex geological and hydrogeological setting. In this study, a hillside situated in Lantau, Hong Kong, was chosen to implement a full-scale, well-instrumented, two-year field monitoring programme subjected to seasonal climatic variations. The instrumentation covered the measurements of the two stress-state variables (i.e., net normal stress and matric suction) in the unsaturated ground, including pore-water pressure (PWP), volumetric water content (VWC), subsurface total horizontal stress, and horizontal displacement. This sophisticated and comprehensive instrumentation scheme may perhaps be the first trial to apply to a natural saprolitic hillslope. The monitoring data from each instrument is reported in this paper. Through the understanding of the interpreted field data, a site-specific geological and hydrogeological model is then established in an attempt to capture the hillslope behaviour as well as the landslide triggering mechanism under severe rainstorms.

Description of study area

The selected hillslope in this study is located at Lantau Island, Hong Kong. Interpretation of aerial photographs from years 1963 to 2004 and engineering geological and geomorphological field mapping are carried out. The geomorphological setting and drainage characteristic of the study area are shown in Fig. 1. Detailed description of the study area is reported by GEO (2007) and is briefly summarized in the following paragraphs.

The natural terrain is moderately to densely vegetated. The terrain itself forms a blunt ridgeline located between a major stream channel on its northeastern side and a shallow topographic valley to the south and west. As a result, runoff from the northeast- and northwest-facing slopes may quickly enter the stream channels at the toe of the hillslope. Although limited mapping of the ground was carried out at the lower portion of the study area, because of its extremely densely vegetated thick ground cover, the shallow gradient of the slope indicated that it was a depositional area with colluvial material. At the mid-portion of the study area, the topography itself formed a very slight bowl-shaped depression, flanked by shallow ridges on either flank and a concave break of slope at the crest and convex break of slope at the toe. This shallow topographic depression may hence constrain any runoff at the central portion of the study area.

Fig. 3. Preliminary geological model for (*a*) section A–A and (*b*) section B–B.

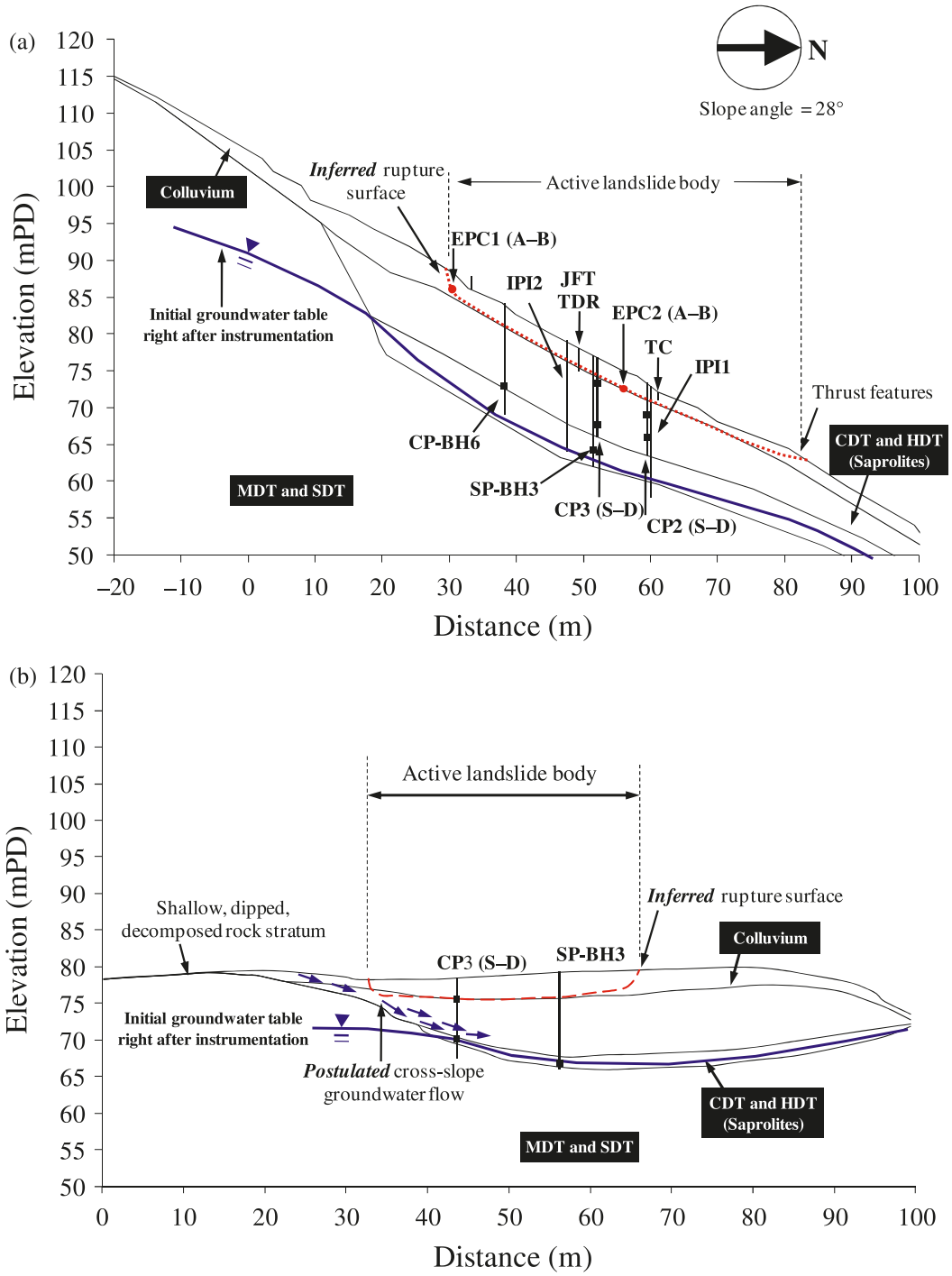

Some prominent features of the active landslide body were identified at the mid-portion of the study area, and details are described in the next section.

Features of active landslide mass

To characterize the geological profile and groundwater condition in the hillslope, fieldworks including drillholes and trial trenches exploration and a geophysical survey were carried out. The locations of the drillholes (BH 1, 3, 5–8) and trial trenches (TT 1–5) are shown in Fig. 1. In particular, the trial trenches were intentionally excavated across the prominent features of the active landslide body in continuity with the aerial photograph interpretation and field mapping.

As shown in Figs. 1 and 2, a series of subparallel tension cracks contouring the hillside of approximately 45 m wide was identified at an elevation between +84 and +86 mPD (mPD is a surveying term in Hong Kong, which stands for "metres above Principle Datum" and refers to the height above mean sea level, approximately 1.23 m above the PD

Table 1. Summary of the measured index properties of the colluvium and the CDT.

Measured index properties	Colluvium	CDT
In situ dry density (kg/m^3)	1504	1600
In situ water content by mass (%)	20.1	17.3
In situ void ratio	0.82	0.68
Specific gravity	2.73	2.68
Liquid limit (%)	41	34
Plastic limit (%)	17	20
Plasticity index (%)	23	14
Gravel content (≥2 mm, %)[a]	0–35	0
Sand content (2 mm – 63 μm, %)[a]	20–25	35
Silt content (2–63 μm, %)[a]	30–50	40
Clay content (≤2 μm, %)[a]	15–25	25
Unified Soil Classification System (USCS)[b]	CL	CL

Note: CL, inorganic silty clay of low to medium plasticity.

[a]Refers to the particle-size distributions in Fig. 4.

[b]ASTM 2006.

Fig. 4. Particle-size distributions of colluvium and CDT.

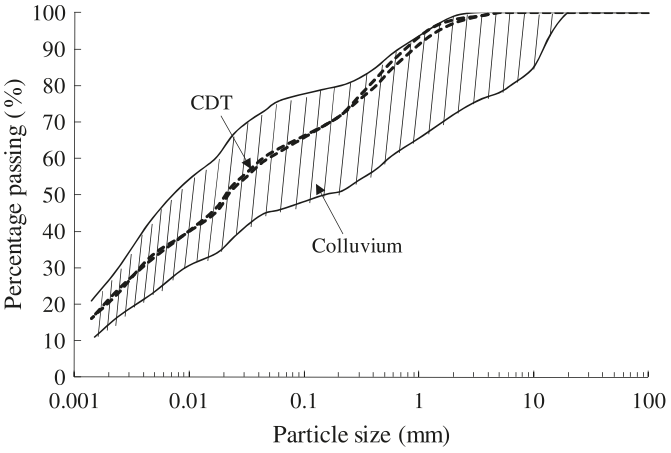

Fig. 5. In situ SDSWCCs of colluvium (Col) and CDT subjected to two wetting–drying cycles (data from Ng et al. 2011).

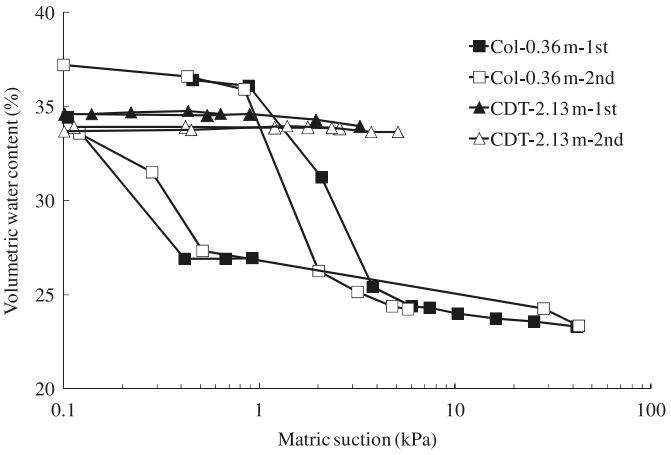

(SMO 1995)) and formed the main scarp features. Trial trenches TT 4 and TT 5 excavated across the subparallel main scarps identified some poorly defined rupture surfaces at shallow depths of about 0.5 m. A number of lateral tension cracks extend north from the main scarps running down the slope from the eastern and the western side of the mid-portion of the study area. Trial trench TT 2 excavated across the eastern flank revealed that some cracks continue down to link the relict joint within highly decomposed tuff (HDT) at about 2 m depth. Moreover, foliations identified in the decomposed tuff at 2 m below ground level (bgl) were slightly oblique to the dip of the hillslope, which indicates significant past ground movements. Besides, a major thrust feature was found at +64 mPD, while some smaller thrust features are identified on both landslide flanks at +76 mPD.

An active landslide body crossing approximately 45 m wide is inferred at the mid-portion of the study area, with slope inclination of about 28°. The identified subparallel main scarps features, the lateral tension cracks, and the thrust features characterize the head, the flank, and the toe of the landslide body, respectively. Field mapping revealed that the past movements of the landslide body were oblique inwards from its flanks and towards its centre and the toe of the hillslope, resulting in the ground destabilization around the landslide flanks and causing distress in the area beneath the lower of the subparallel main scarps.

Geological–hydrogeological model

Fieldworks including drillholes exploration and geophysical survey aimed to identify the geological profiles, in situ soil properties, and groundwater conditions of the natural hillslope. Some key descriptions of the superficial and solid geology are summarized as follows. Colluvial materials, which comprised mainly sand and silt with some angular to subangular gravel- and cobble-sized rock fragments, were encountered at the superficial region. A relatively thick layer of colluvial deposits up to 3 m was found within the topographic depression at the mid-portion of the study area. The underlying saprolite is typically described as extremely to moderately weak, light grey, dappled light brown, completely decomposed coarse ash tuff (CDT, completely decomposed tuff) or HDT with occasional angular and subangular fine gravel.

For the solid geology, moderately strong, grey and

Fig. 6. In situ permeability functions of (*a*) colluvium (Col) and (*b*) CDT subjected to two wetting–drying cycles (data from Ng et al. 2011). R1, range of saturated permeability of colluvium (2×10^{-6} to 9×10^{-4} m/s) according to GCO (1982); R2, range of saturated permeability of CDT (3×10^{-6} to 9×10^{-6} m/s) according to GCO (1982).

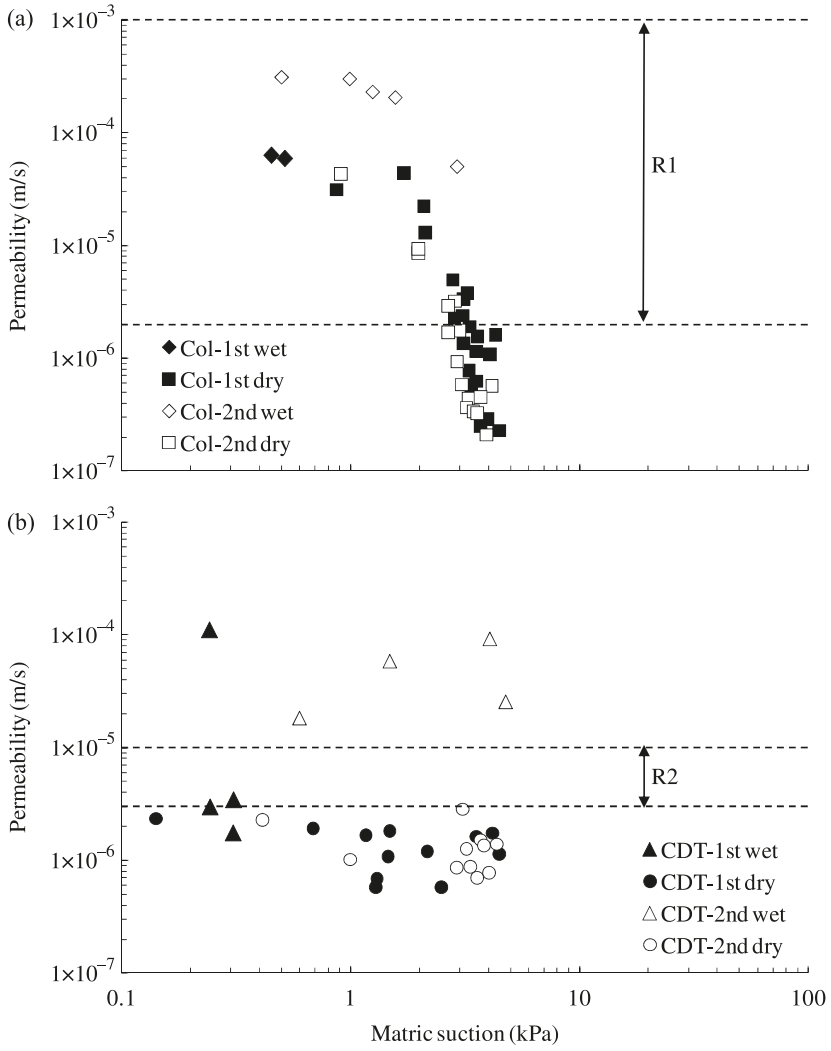

Table 2. Some detailed information about each instrument.

Instruments	Measurements	Installation depth (m bgl)	Measurement range	Source
Tipping-bucket rain gauge	Rain depth	N/A	0–500 mm/h	Campell Scientific
Jet-filled tensiometer	PWP	0.5, 1.5, 2.5	0 to –90 kPa	Soilmoisture Equipment Corp.
Heat dissipation matric water potential sensor	Measure temperature changes and deduce matric suction through calibration curve	0.2, 0.4, 0.6	10–2500 kPa	Campbell Scientific
Water content reflectometer	Measure period and deduce VWC through calibration curve	0.5, 1.5, 2.5	0–50%	Campbell Scientific
Casagrande-type piezometer	Measure positive PWP	Refer to Table 3	0–350 kPa	Dataqua Elektronikai Ltd.
Vibrating-wire earth pressure cell	Measure wire frequency and deduce total horizontal stress	2	1–350 kPa	Geokon
In-place inclinometer	Measure inclined angle and deduce horizontal displacement	0, 1, 3, 5, 7	15°	Geokon

Table 3. Installation records of standpipes and Casagrande-type piezometers.

Instruments		Response zone			
Type	Symbol	From (m bgl)	To (m bgl)	Ground level (mPD)	Material around the response zone
Standpipe	SP-BH3[a]	3.00	15.10	77.43	CDT and HDT
	SP-BH5	3.00	12.53	84.33	MDT to SDT
	SP-BH7	3.00	10.20	97.77	MDT to SDT and thin bands of HDT
	SP-BH9	3.00	12.72	114.25	MDT to SDT
Casagrande-type piezometer	CP-BH1[b]	14.02	15.32	58.90	HDT with a zone of fractured MDT
	CP-BH6	10.70	12.00	84.55	Interface of HDT and MDT
	CP1S	3.70	5.00	60.74	HDT to MDT
	CP1D	8.00	9.30		Competent bedrock strata
	CP2S	3.70	5.00	73.35	Interface of CDT to HDT
	CP2D	7.05	8.35		Interface of CDT to HDT
	CP3S	3.70	5.00	77.22	Colluvium
	CP3D	8.70	10.00		CDT to HDT

[a]SP-BH3 means that a standpipe was installed in the drillhole BH 3.
[b]CP-BH1 means that a Casagrande-type piezometer was installed in the drillhole BH 1.

Fig. 7. Variation of PWP with time during rainstorms (*a*) 18–22 April and (*b*) 5–9 June 2008; variation of VWC with time during rainstorms (*c*) 18–22 April and (*d*) 5–9 June 2008.

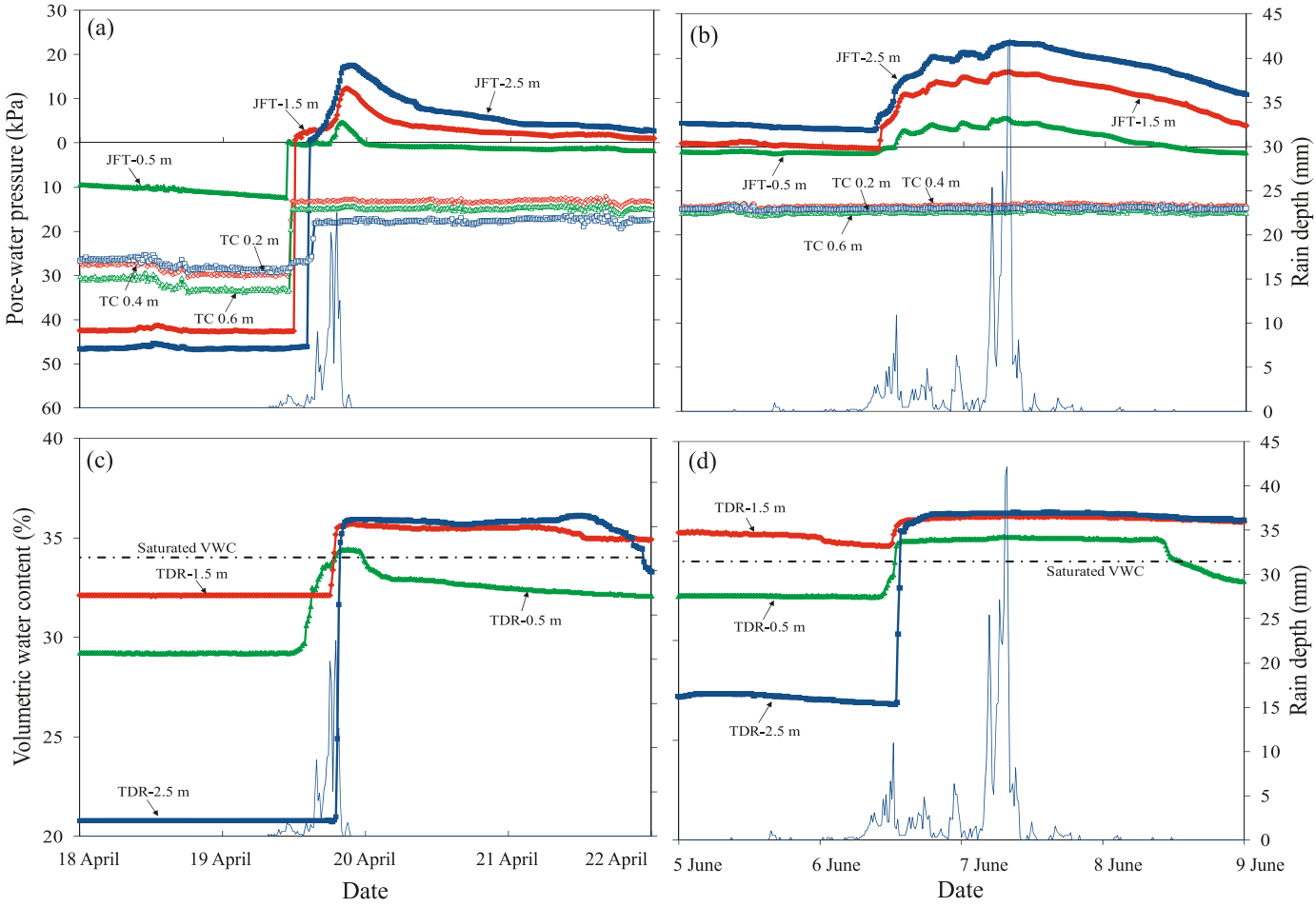

dappled light brown, slightly or moderately decomposed coarse ash tuff (SDT, slightly decomposed tuff; MDT, moderately decomposed tuff) was encountered beneath the saprolites. Closely spaced to medium-spaced rock joints were kaolin infilled. Evidence of hydrothermal alteration (silicification and honeycomb weathering of feldspar minerals) of MDT, which is considerably more resistant to weathering than the surrounding rock, was mainly identified in drillhole

Fig. 8. Variation of piezometric level with time during rainstorms (*a*) 18–22 April and (*b*) 5–9 June 2008.

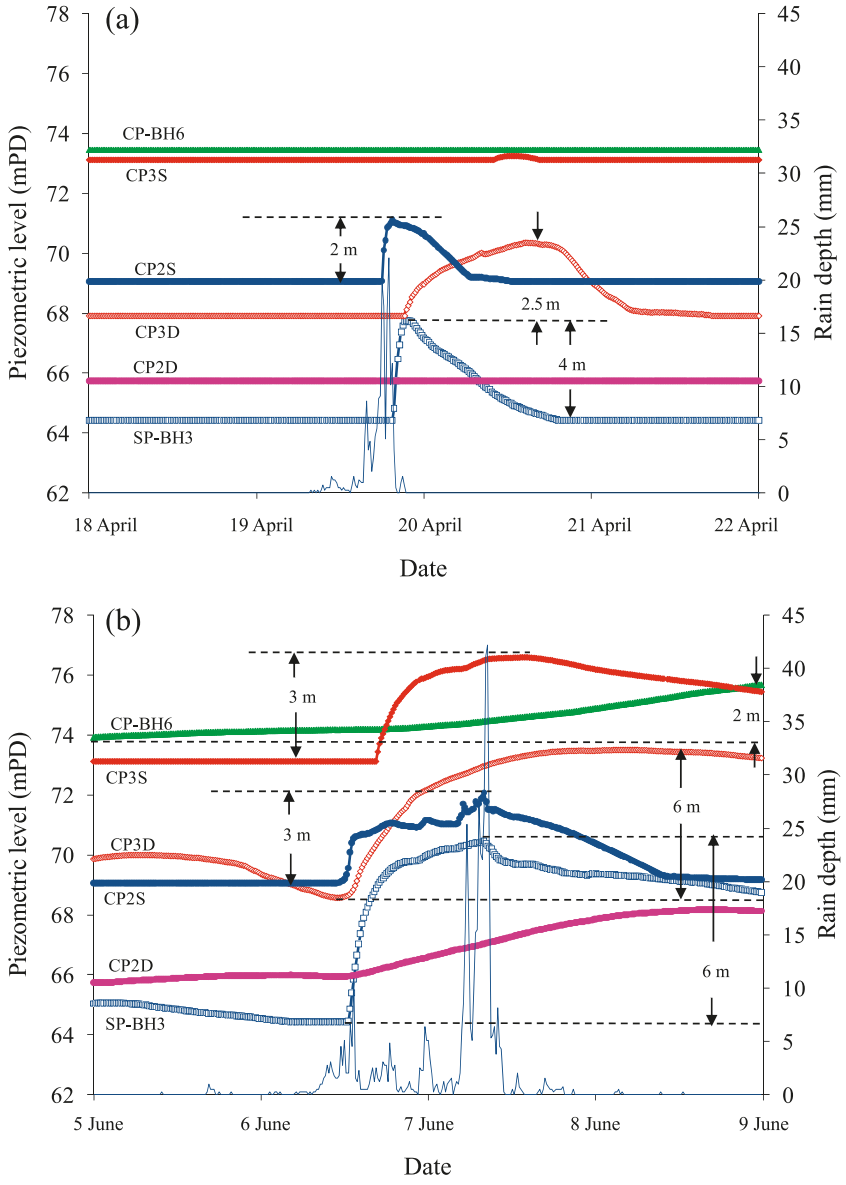

BH 5 (near the western landslide flank) below depths of 1.7 m and in drillhole BH 8 (near the eastern landslide flank) between the depths of 8 and 12 m (see Fig. 1). The drop of the rock head level from the western landslide flank to the eastern one possibly causes the formation of bowl-shaped localized depression at the central portion of the landslide body and may as a result exert certain impact on the hydrogeological regime.

Based on the limited field records, a preliminary and simplified geological profile is established and is shown in Fig. 3 for section A–A and B–B. The groundwater profile right after instrumentation generally followed that of the MDT and was about 1–2 m above the decomposed rock head surface. The inferred rupture surfaces are also shown for reference. According to the classification system of the types of slope failure by Varnes (1978), the active landslide body in this study area appears to undergo a retrogressive translational-slide type of failure of limited mobility along some poorly defined rupture surfaces at 3–5 m bgl, which are just beneath the colluvium–CDT interface.

Soil properties

A series of conventional laboratory tests were conducted to determine the soil properties of both the colluvium and the CDT. They included the determination of specific gravity, in situ void ratio, in situ dry density and water content, and the Atterberg limits. The measured index properties are summarized in Table 1. As determined by the sieve and the hydrometer analysis (BSI 1990), the particle-size distributions of each material obtained from some block samples are shown in Fig. 4. It can be seen that both materials are dominated by the silt content (about 40% each), while both sand and clay content is less than 35%. To further characterize the in situ unsaturated hydraulic properties of the collu-

Fig. 9. Variation of in situ total horizontal stress with time near main scarps (EPC1) during rainstorms (*a*) 18–22 April and (*b*) 5–9 June 2008; variation of in situ total horizontal stress with time at central portion of landslide body (EPC2) during rainstorms (*c*) 18–22 April and (*d*) 5–9 June 2008.

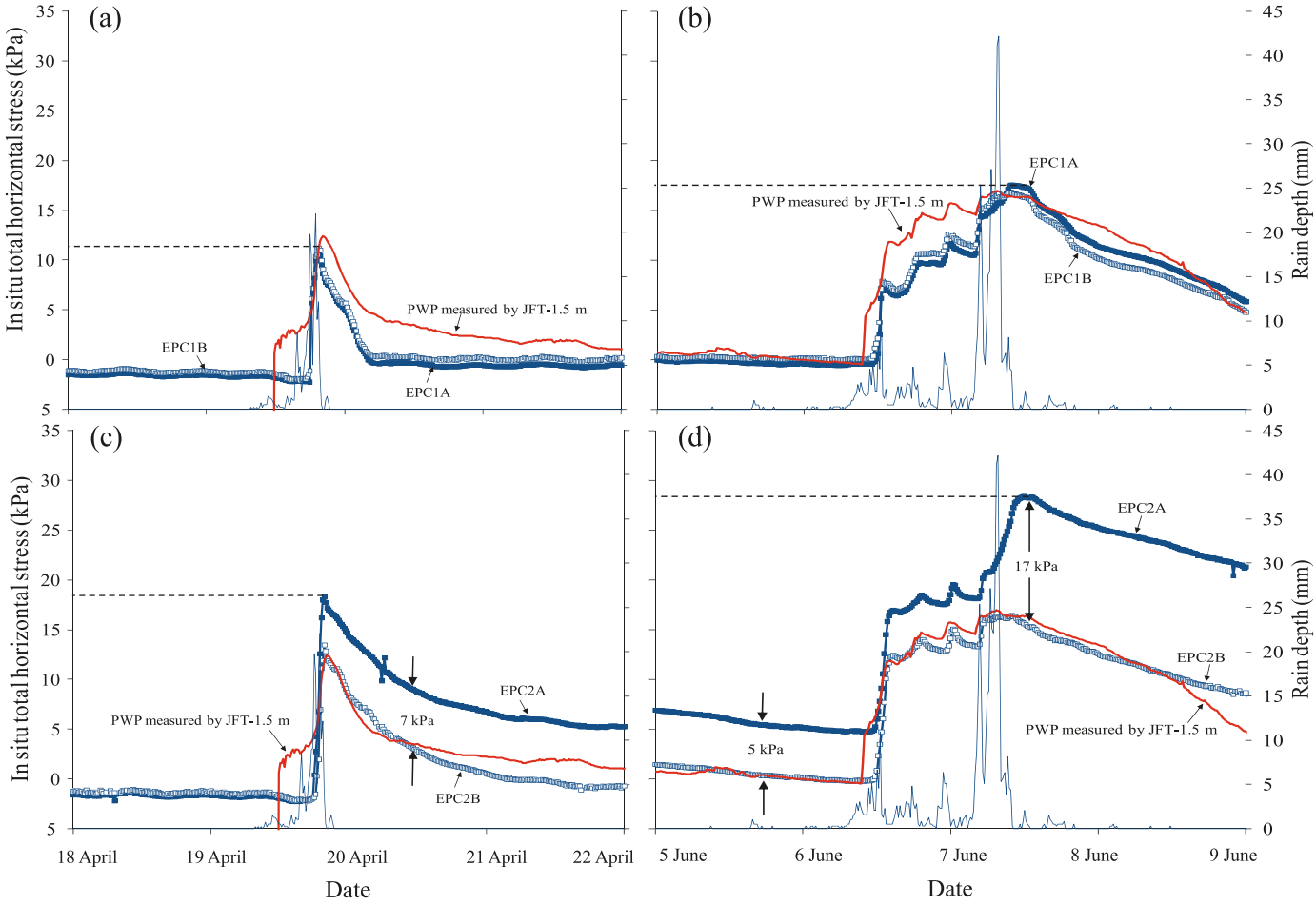

vium and the CDT, the instantaneous profile test (IP test) was conducted at the toe of hillslope (see Figs. 1 and 2) prior to the commencement of the field monitoring (Ng et al. 2011). Figures 5 and 6 show the measured in situ stress-dependent soil-water characteristic curves (SDSWCCs) and permeability function subjected to two wetting–drying cycles of each material, respectively. Detail discussions of these hydraulic properties for each material are reported by Ng et al. (2011) and are not repeated in this paper.

Instrumentation programme and monitoring results

A comprehensive instrumentation scheme was implemented in this field monitoring programme. The instruments consisted of jet-filled tensiometers (JFTs), water content reflectometers (TDRs), heat dissipation matric water potential sensors (TCs), vibrating-wire earth pressure cells (EPCs), in-place inclinometers (IPIs), Casagrande-type piezometers (CPs), standpipes (SPs), and a tipping-bucket rain gauge (RG). These instruments were typically installed around the active landslide body. The schematic instrument arrangement is shown in Figs. 2 and 3. Detailed information of each instrument is summarized in Tables 2 and 3. The sampling frequency of each instrument was 15 min. Since all instruments recorded significant responses during the two heavy rainstorms from 18 to 22 April and from 5 to 9 June 2008, the monitoring results between these two periods are selected to investigate the hillslope behaviour in this paper.

Rainfall characteristic

A RG was installed to record rain depth and to estimate rainfall intensity. Although the area for sampling is comparatively small when compared to that of the terrain, it is assumed that the measured rain depth is representative and uniform over the entire study area. In comparisons with the rainfall isohyet and the monthly rainfall amount reported by the Hong Kong Observatory (HKO), the measurements made by the RG are generally consistent and have reliable quality.

The recorded annual rainfall in 2008 was about 3084 mm. The wet season started in mid-April. It brought Hong Kong heavy rain on 19 April, with maximum 24 h rolling rainfall of 187.7 mm (i.e., peak rainfall intensity of 62 mm/h). It necessitated the issuance of the first Black Rainstorm Warning (i.e., hourly rainfall exceeds 70 mm) by the HKO in 2008. In June, the weather was marked with heavy rains and squally thunderstorms. The RG recorded the rain depth of

Fig. 10. Down-slope displacement profiles of (*a*) IPI2 and (*b*) IPI1; cross-slope displacement profiles of (*c*) IPI2 and (*d*) IPI1 at central portion of active landslide body.

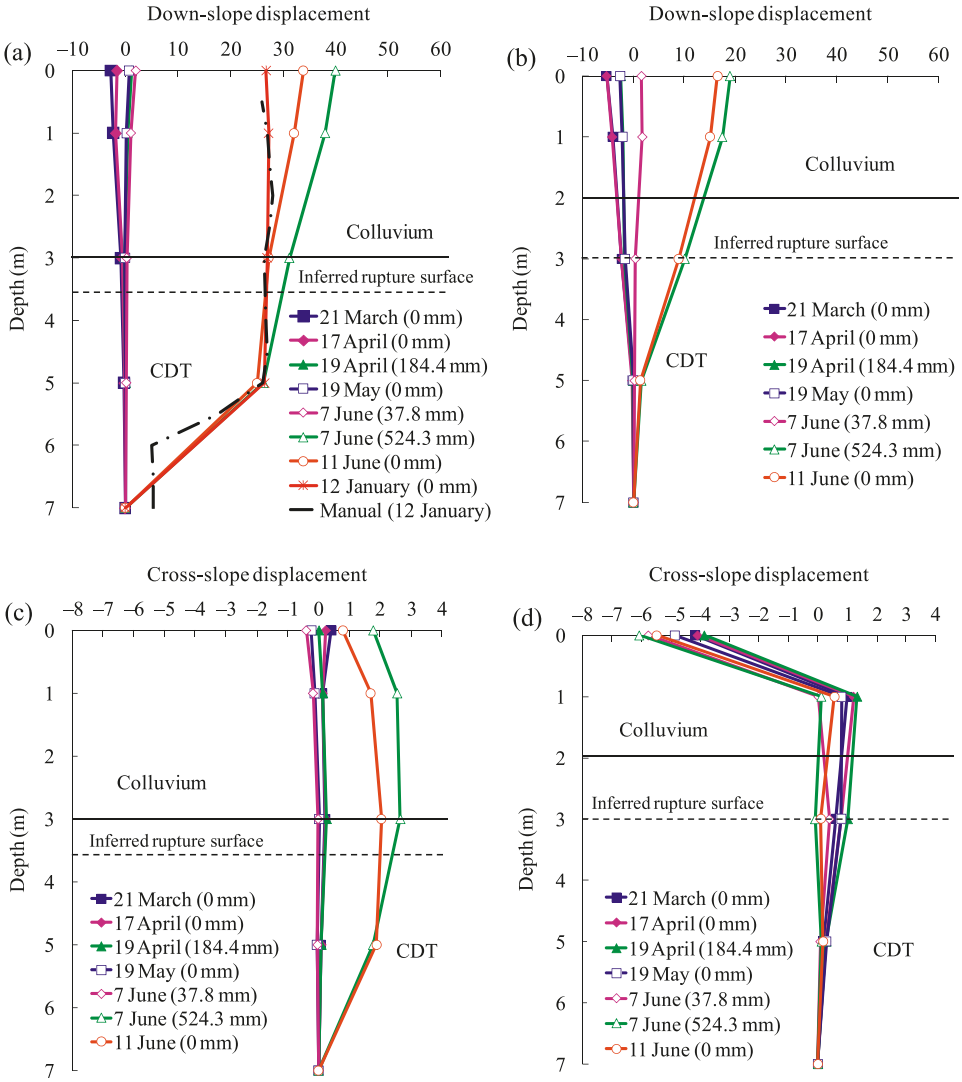

1391 mm (45% of the annual rainfall in 2008) over the month. The peak 1 h rolling rainfall of 133.5 mm was recorded on 7 June and was the highest since the record began. The return period may be estimated using the procedures described by Evans and Yu (2001) based on the Gumbel method, though the estimation may not be necessarily applicable for other locations in Hong Kong (Peterson and Kwong 1981; Lam and Leung 1994; Evans and Yu 2001). The return period of the peak 4 h rolling rainfall of 323.6 mm on 7 June is approximately 245 years. The passage of the several tropical cyclones from July to October brought continuous storm surges, and the 24 h rolling rainfall was typically about 200 mm.

Response of PWP and VWC

Three pairs of JFTs and TDRs were installed to measure PWPs and VWCs, respectively. Each pair of the instruments was installed at depths of 0.5, 1.5, and 2.5 m bgl near the subparallel main scarps (see Fig. 2). Each TDR measures the travelling time of an applied electrical pulse along the rods. The travelling time primarily depends on the dielectric constant of the water in the surrounding soil, and VWC can thus be deduced through a soil-specific calibration curve indirectly. Each JFT and TDR was inserted into a 50 and 100 mm diameter predrilled hole, respectively. In particular, the rods of each TDR were carefully inserted into the ground to avoid any damage of sensors. After installation, the lower part of each predrilled hole was backfilled with a 100 mm thick layer of compacted in situ soil and followed by bentonite cement grout. According to the drillhole records, instruments embedded at 0.5 and 1.5 m bgl were situated within the colluvium while instruments embedded at 2.5 m bgl were situated within the CDT.

The measurement range of JFTs is limited to about 80 kPa of negative PWPs because of the possibility of cavitation. Three calibrated TCs were installed in the colluvial deposits at 0.2, 0.4, and 0.6 m bgl. According to the manufacturer (CSI 2009), each TC is supposed to measure matric suction indirectly between 10 and 2500 kPa, and its resolution is claimed to be up to 1 kPa at suction greater than

Fig. 11. Hillslope responses at peak rain depth on 7 June 2008.

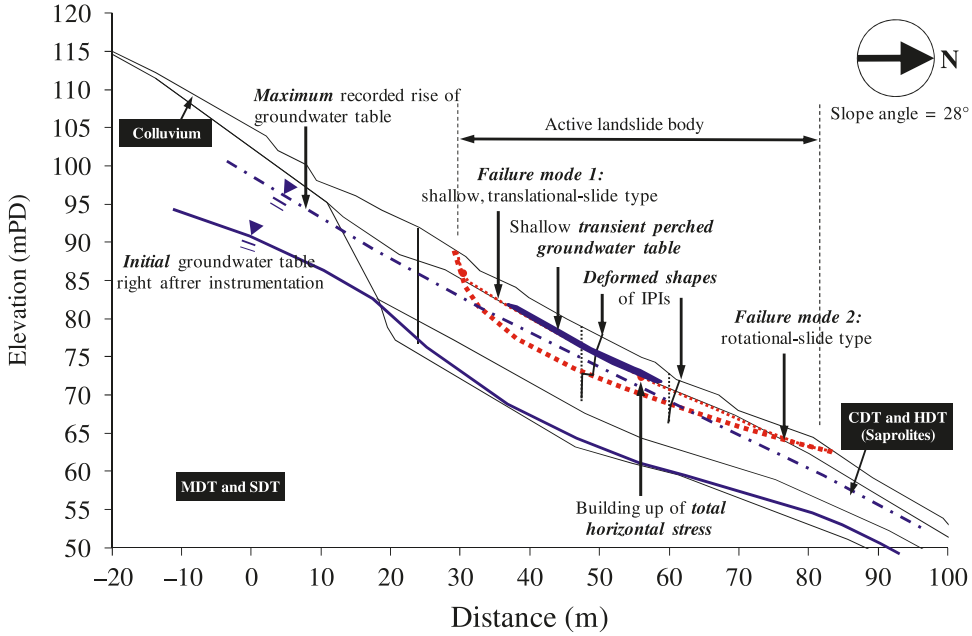

100 kPa. Depending on the thermal conductivity of the ceramic–water complex surrounding the sensor, temperature changes under constant power dissipation from the line heat source are measured at a specified sampling frequency. Matric suction can then be deduced by each TC through a soil-specific calibration curve indirectly. To have reasonable comparisons with the JFT measurements, matric suctions deduced by the TCs are expressed in terms of PWP, assuming that pore-air pressure is equal to the atmospheric pressure.

Figure 7 shows the variation of PWP and VWC in responses to the two rainstorms from 18 to 22 April and from 5 to 9 June 2008. The PWPs measured by the JFTs have been corrected to account for the elevation head difference between the ceramic tip and the pressure transducer. Hence, maximum positive PWPs of 5, 15, and 25 kPa can be deduced for JFT installed at 0.5, 1.5, and 2.5 m bgl, respectively. Matric suction deduced from each TC is temperature corrected. As shown in Figs. 7*a* and 7*c*, the PWPs initially decreased from –10 to –45 kPa with depths, while the VWCs increased from 21% to 32% with depths. For the rainstorms of 19 April, the PWPs at all depths increased promptly to about 0 kPa within 30 min. This rapid advancement of wetting front seemed physically impossible for the colluvium, having an average saturated permeability of approximately 10^{-7} m/s (see Fig. 6), to seep 2.5 m depth within a short period of time. Similar rapid increases of PWP during rainfalls can be observed from other in situ PWP measurements carried out by Gasmo et al. (1999), Ng et al. (2003), and Ng et al. (2011) when using JFTs.

At the peak rain depth on 19 April, positive PWPs were deduced at all depths, approaching a full hydrostatic condition at the ground surface (see Fig. 7*a*). Besides, the PWPs deduced by the three TCs decreased from about –28 kPa to a minimum value of –15 kPa consistently. It is noted that when the soil moisture is too high, the change of water thermal conductivity in the ceramic of each TC becomes indistinguishable. According to the calibration carried out in the laboratory, it is found that when PWP is less than –60 kPa, the maximum deviation from the calibration curve and the precision of each TC is ±20% and 13 kPa, respectively. Therefore, any measurement made by each TC is expected to be less accurate for PWP smaller than –60 kPa. On the other hand, substantial but gradual increases of VWC are observed at depths of 0.5 and 1.5 m (see Fig. 7*c*). The fairly close agreement with the laboratory-measured saturated VWC (34%) implies that ground above 1.5 m bgl may approach its saturation limit. In contrast, the observed rapid increase of VWC at 2.5 m bgl (from 21% to 36% within 30 min) seems to indicate the problematic installation of the TDRs. Air pockets may possibly form if the rods of TDRs are not fully inserted to a ground that is stiff or contains frequent gravels, cobbles, and boulders.

During the heavy rainstorms from 5 to 9 June, the responses of PWPs and VWCs generally exhibited similar features to those observed in the previous rainstorms (see Figs. 7*b* and 7*d*). Significant positive PWPs were deduced at all depths. This full hydrostatic condition at ground surface is rare but sometimes observed, which again suggests the problematic installation technique for the JFTs. Constant minimum PWP of –15 kPa was deduced by all the three TCs during the entire rainstorms. Besides, the increase of VWC at 0.5 and 1.5 m bgl was gradual and limited, attaining a maximum value of about 36.5%.

Piezometric-level variation

The SPs and CPs were installed at various elevations around the active landslide body to monitor the variations of the piezometric level. They aimed to record any response of the groundwater table and any formation of transient perched groundwater tables during rainstorms. Each SP consisted of an open-ended, perforated PVC tube, where the gap between the tube and the drillhole wall was backfilled with gravel filter. The response zone was typically from about 3 to 12 m bgl. On the other hand, a pressure transducer

equipped in each CP was protected by a perforated rigid sheath, and the sheath was wrapped by a sand filter for backfilling. The response zone of CP was narrower when compared to SP and commonly ranges from 1.5 to 2 m in height. Among the CPs, the CP1, CP2, and CP3 consisted of a shallow device (S) and a deep device (D), which were installed in a single drillhole. Table 3 summarizes the elevation and the range of the response zone of each SP and CP. The material surrounding each response zone is also shown for reference.

Focusing on the groundwater responses within the active landslide body, the SP-BH3, CP-BH6, CP2S, CP2D, CP3S, and CP3D are selected for detailed assessment in this paper. The variation of piezometric level, i.e., elevation head plus pressure head, during the rainstorms from 18 to 22 April and from 5 to 9 June 2008 are shown in Fig. 8. It should be noted that any change of piezometric level indicates change of positive PWP head. As shown in Fig. 8*a*, at the peak rain depth on 19 April, the shallower device CP2S recorded substantial increase of piezometric head of 2 m while the deeper device CP2D did not respond. On the other hand, the piezometric head in the SP-BH3 increased by 4 m and dropped back to its tip level in a gradual manner within 1 day. The CP3D, which was installed at nearly the same elevation as SP-BH3 (see Table 3 and Fig. 3*b*), recorded consistent and similar variations but with less increase of piezometric head (about 2.5 m). However, surprisingly, the shallower device, CP3S, showed negligible response, indicating a complex hydrogeological regime in the hillslope. The groundwater flow mechanism might be primarily affected by the geological setting of this particular hillslope and is discussed in detail later.

During the heavy rainstorms from 5 to 9 June, all of the devices typically showed significant increase of piezometric head and dropped gradually after the peak rain depth (see Fig. 8*b*). In particular, both the CP2S and the CP3S recorded a peak increase of piezometrical head of 3 m while the CP-BH6 exhibited a gradual and limited increase of 2 m. The SP-BH3 and CP3D again showed comparable piezometric head increases of 6 m at deep regions because of their similar installation depth. These dramatic increases of water pressure may also be affected by the complex geological setting of the natural hillslope.

Subsurface total horizontal stress

Two pairs of EPCs were installed near the main scarps (EPC1) and at the central portion of the landslide body (EPC2) to monitor the total horizontal stress at 2 m in depth (see Figs. 2 and 3*a*). For each pair, the variations of total horizontal stress in both the down-slope (A) and the cross-slope (B) direction were recorded. Each EPC was inserted in a narrow slot, which was slightly oversized at the base of a trial pit at 2.5 m bgl. The resulting void between the CDT and the sensor was then backfilled with cement bentonite grout.

Figure 9 shows the variation of in situ total horizontal stress with time in responses to the rainstorms from 18 to 22 April and from 5 to 9 June 2008. The deduced positive PWPs recorded by the JFT-1.5 m are also shown for comparison. Initially, a few negative values (i.e., tensile stresses) of 0.5 kPa were recorded, which was probably due to the stress alteration during installation and (or) shrinkage of grout. Nevertheless, these negative readings are apparent, since the accuracy of EPCs is ±0.35 kPa (Geokon 2007*a*). As shown in Figs. 9*a* and 9*b*, the measured total horizontal stress of EPC1A and EPC1B recorded extremely similar variations during the two rainstorms. Peak total horizontal stresses of 12 and 18 kPa were attained at peak rain depths on 19 April and 7 June, respectively. The stress then dropped gradually and stabilized at a slightly larger pressure as both the rainstorms cease. Moreover, it can be seen that the measurements made by the EPC1A and (or) EPC1B were reasonably close to the positive PWPs deduced by the JFT-1.5 m. Theoretically, it is anticipated that decrease of matric suction would consequently result in elastic soil swelling. However, the above observations seem to suggest that the increases of stress near the main scarps were likely caused by the increase of positive PWPs instead of the earth pressure itself. In other words, the backfilled cement bentonite grout may possibly strengthen the ground and thus reduce its compressibility upon matric suction changes.

At the central portion of the active landslide body, the trend of the measured total horizontal stress at both orientations (EPC2A and EPC2B) were similar, and the magnitude in the down-slope direction was consistently larger than that in the cross-slope direction after rainstorms (see Figs. 9*c* and 9*d*). At peak rain depths on 19 April and 7 June, the maximum total horizontal stresses in the down-slope direction were 18 and 28 kPa, respectively. The stress difference between orientations increased from about 0 to 7 kPa on 19 April and from 5 to 17 kPa on 7 June. The stresses recorded by both the EPC2A and EPC2B dropped steadily as the rainstorms ceased. Moreover, it can be seen that the variations of the total horizontal stress recorded by both the EPC1B and EPC2B are close to the positive PWPs deduced by the JFT-1.5 m (see Figs. 9*b* and 9*d*). It suggests that the stress changes in the cross-slope direction in the active landslide body were likely originated by the increase of positive PWPs. On the contrary, the larger stress changes recorded by the EPC2A in the down-slope direction indicate either significant ground movement or the presence of preferential groundwater flow in the down-slope direction.

Subsurface horizontal deformation characteristic

Two IPIs (IPI1 and IPI2) were installed around the central portion of the active landslide body for subsurface horizontal displacement measurements. Four tilt sensors were scheduled to suspend "in-place" along each inclinometer casing at ground surface (i.e., 0 m bgl), 1, 3, and 5 m bgl. The horizontal displacement at 7 m bgl was assumed to be zero. The tilt sensors of each IPI continuously recorded the inclined angle as a result of ground deformation, with accuracy of 0.015° (Geokon 2007*b*). Similar to the EPCs, horizontal displacement in both the down-slope and the cross-slope direction were monitored.

Figure 10 shows the down-slope and cross-slope horizontal displacement profiles of IPI1 and IPI2 on some key days. The numbers shown in parentheses denote the peak rain depth during the day. The estimated colluvium–CDT interface and the location of the inferred rupture surfaces as revealed from the ground investigations are shown on the displacement profiles for comparison (see also Fig. 3*a*). During the rainstorms from 18 to 22 April, the ground generally exhibited "cantilever"

mode of deformation towards the down-slope direction. The peak displacement change at the ground surface was approximately 3 mm (see solid triangular symbol in Figs. 10*a* and 10*b*). This deformation characteristic is consistent with the inferred shallow, translational-slide type of failure, where the rupture surfaces are just below the interface between the colluvium and the CDT.

In responses to the heavy rainstorms from 5 to 9 June, significant down-slope ground movements were recorded for both the IPI1 and IPI2 (see open triangular symbol in Figs. 10*a* and 10*b*). In particular, the IPI2 measured a nearly irrecoverable displacement change of 40 mm, and the displacement profile was fairly uniform along the depth. There is hence possibility that the movement in the upper soil profile drags the lower portion of the casing. The assumption of zero horizontal displacement at 7 m bgl may be questionable and needs to be examined in this circumstance. A conventional manual inclinometer survey was therefore undertaken to accurately record the "real" deformation profiles. The manual measurement was made on 9 January 2009 and is compared with the displacement recorded on the same day (see dotted line and cross symbol in Fig. 10*a*). The comparison provides evidence that well-defined rupture surfaces situated at 5 m bgl or deeper have possibly been developed because of the relatively large displacement between 5 and 7 m. In contrast, the ground displacement recorded by the IPI1 exhibited a cantilever mode of deformation when the peak rain depth occurred on 7 June (see Fig. 10*b*). The peak displacement increment at the ground surface was found to be 25 mm.

In contrast to the ground movements in the down-slope direction, the displacement change in the cross-slope direction appears to be limited and less sensitive to the rainstorms (see Figs. 10*c* and 10*d*). The ground generally tended to deform towards the easterly direction, where the maximum displacement of 3 mm took place near the colluvium–CDT interface (see open circle and open triangle symbols in Fig. 10*c*). Consistent to the observations recorded by the groundwater monitoring devices (see the variations of the SP-BH3, CP3S, and CP3D in Fig. 8), this unusual deformation characteristic might be affected by the complex groundwater flow and geology of the active landslide body. The detail is discussed in the next section.

Investigation of hillslope behaviour

In an attempt to capture the hillslope behaviour and the landslide triggering mechanism upon precipitations, a site-specific geological and hydrogeological model are established in this section. The field observations during the heavy rainstorms from 18 to 22 April and from 5 to 9 June 2008 are interpreted and comprehended. The site-specific infiltration and deformation characteristics of the hillslope are then identified.

A preliminary geological and hydrogeological model based on the previous ground investigations, field mapping, and aerial photograph interpretation has been set up and is reported and described earlier. The simplified soil profile, initial groundwater table, and the inferred rupture surfaces are shown in Fig. 3. Prior to the rainstorms, the ground above 1.5 m bgl was initially wet, as shown by the fairly close agreement between the field- and laboratory-measured VWC (see Fig. 7*c*). It probably resulted from the considerable amount of antecedent rainfalls from January to March 2008. For the ease of discussions, the hillslope responses and some observed key features at the peak rain depth on 7 June are schematically illustrated in Fig. 11.

Infiltration characteristic and groundwater condition

Upon rainstorms, significant increases of piezometric head and total horizontal stress at 2 m bgl were typically and consistently observed (see the variations of the CP2S and CP3S in Fig. 8 and variations of EPC1 and EPC2 in Fig. 9). Positive PWPs as high as 20 kPa were frequently recorded. The VWCs also showed a gradual but limited increase to attain in situ saturation limits (about 36%) at shallow regions (see Figs. 7*c* and 7*d*). As revealed from the geophysical survey, a lens of stiff material was found to overlay the ground surface of the hillslope. It indicates the presence of corestones or fractured decomposed rock material as a result of past mass wasting processes. Based on these field observations and measurements, shallow (i.e., top 3 m) transient perched groundwater tables are believed to be developed within the bouldery colluvial deposit in the landslide body (see Fig. 11). This is consistent with the observation from the IP test that positive PWPs were recorded near the colluvium–CDT interface, likely because of the significant difference of unsaturated water permeability between the two strata (Ng et al. 2011; see also Fig. 6).

During the rainstorms from 18 to 22 April, the significant increase of piezometric head of about 4 m (40 kPa of positive PWP) at 10 m bgl (see the variations of the SP-BH3 in Fig. 8*a*) implies the possible rise of the main groundwater table, resulting from the continuous advancement of rainwater in the subsurface. As shown in Fig. 3*b*, a shallow decomposed rock stratum dipping towards the easterly direction was identified across the hillslope at +75 mPD. This unusual complex geological setting of this particular hillslope may affect its hydrogeological regime and hence the groundwater flow mechanism upon infiltration. It may be reasonable to postulate that a portion of rainwater infiltrated from the western flank might flow towards the central portion of the landslide body on top of this dipped rock head profile, resulting in possible cross-slope groundwater flow (see the arrows in Fig. 3*b*).

As indicated by the close field- and laboratory-measured VWC, the ground is believed to be significantly wetted after the rainstorms in April (see Fig. 7*d*). The increase of PWP (or decrease of matric suction) (see Fig. 7*b*) increased hydraulic flow paths in the ground, and its water permeability would hence be increased (see Fig. 6). The "improvement" of ground permeability would thus allow more rainwater to seep in the subsurface during the subsequent rainstorms from 5 to 9 June. As a result, at the peak rain depth on 7 June, the main groundwater table probably rose by 6 m from the initial position (see the variations of the SP-BH3 and CP3D in Fig. 8*b*), approaching the colluvium–CDT interface (see Fig. 11).

Deformation characteristic and failure mode

The increases of total horizontal stress (see Figs. 9*c* and 9*d*) resulting from the building up of positive PWPs at shallow regions (see the variations of the three JFTs in Figs. 7*a* and 7*b* and variations of the CP2S and CP3S in Figs. 8*a* and

8*b*) during rainstorms would likely result in soil deformation. According to the measured horizontal displacement, two distinct modes of deformation were identified in this hillslope (see Figs. 10*a* and 10*b*). At the peak rain depth on 19 April, a cantilever mode of deformation with limited displacement (about 3 mm at the ground surface) was observed. This deformation characteristic suggests that the inferred shallow translational-slide type of movement along some poorly defined rupture surfaces at 3–5 m bgl, which is near the colluvium–CDT interface, is likely reactivated (failure mode 1 in Fig. 11).

In response to the heaviest rainfall on 7 June, well-defined rupture surfaces have possibly been developed at 5 m bgl or deeper at the central portion of the landslide body. A nearly irrecoverable lateral displacement of 40 mm was recorded at the ground surface (see Fig. 10*a*). This observed "deep-seated" mode of deformation is probably the consequence of the significant increases of total horizontal stress (maximum value of 28 kPa) in the down-slope direction (see the variation of the EPC2A in Fig. 9*d* and Fig. 11). By comparing the measured data on 7 June 2008, 11 June 2008, and 12 Jan 2009 as shown in Fig. 10*a*, it is interesting to note that there were some recoverable displacements recorded after the heavy rainstorm on 7 June 2008. Similarly, some partial recoverable displacements were also reported by Ng et al. (2003) from their field monitoring of an unsaturated expansive soil slope. The deep-seated mode of slope movement implies that the landslide mass underwent another distinct type of failure mode. Considering the field-observed discontinuities like relict joints and foliations in the subsurface, a rotational-slide type of failure may have been triggered (failure mode 2 in Fig. 11). According to the classification system of the types of slope failure by Varnes (1978), the combined failure mode (failure modes 1 and 2 in Fig. 11) of the landslide body may be described as multiple, translational-slide, and rotational-slide type.

Apart from the effects of stress changes upon precipitations, the existence of the unusual complex geological setting may also influence the deformation characteristic of the landslide body. The possible cross-slope groundwater flow on the shallow, dipped decomposed rock head regime at +75 mPD (see Fig. 3*b*) might result in notable easterly horizontal ground movements. The maximum displacement change of about 3 mm took place at 3 m bgl, which is close to the colluvium–CDT interface (see Fig. 10*c*). The measurement suggests that the landslide body tended to slide towards the easterly direction upon failure.

Summary and conclusions

The behaviour of an unsaturated saprolitic hillslope upon heavy rainstorms was investigated through a comprehensive, full-scale field monitoring programme in Hong Kong. Various types of instruments were installed around the active landslide body to measure the two stress-state variables (i.e., net normal stress and matric suction) and their influences on slope performance. Monitoring results including PWP, VWC, total horizontal stress, horizontal displacement, and rainfall intensity during the two selected heavy rainstorms from 18 to 22 April and from 5 to 9 June 2008 were reported and interpreted. Site-specific geological and hydrogeological models were then established by understanding and comprehending the aerial photograph interpretation, field mapping, ground investigation fieldworks, and interpreted monitoring results.

Except for the measurements made by the JFTs and the TDR installed at a depth of 2.5 m, all instruments generally provided reliable and good quality data. The measurements among each instrument were also shown to have strong correlation.

During the rainstorm of 19 April (peak rainfall intensity of 62 mm/h), the VWC of the overlying colluvium attained an in situ saturation limit of 36%. Shallow pressure transducers installed at 2 m bgl frequently recorded positive PWPs up to 20 kPa, suggesting that transient perched groundwater tables may have been developed within the bouldery colluvial deposit on the top 3 m. The increases of total horizontal stress resulting from the building up of positive PWPs resulted in slope movements. A cantilever mode of ground deformation was observed. This kind of deformation characteristic implies that the shallow translational-slide type of failure (failure mode 1) of the landslide body was likely reactivated. It slid along some poorly defined rupture surfaces at 3–5 m in depth, near the colluvium–CDT interface.

When the rainfall reached its peak intensity on 7 June (133.5 mm/h), the main groundwater table probably rose by 6 m, approaching the colluvium–CDT interface. The groundwater flow mechanism of this particular hillslope may have been affected by its complex geological setting, where a shallow decomposed rock stratum dipping towards the easterly direction was identified across the hillslope. Cross-slope groundwater flow at the central portion of the landslide body might have been possible.

Because of the significant increase of total horizontal stress (maximum value of 28 kPa on 7 June) in the down-slope direction, a deep-seated mode of slope movement resulted. A nearly irrecoverable displacement change of 40 mm was recorded at the ground surface, and the displacement profile was fairly uniform along the depth. Well-defined rupture surfaces were possibly developed at about 5 m below ground or deeper. Considering the identified in situ discontinuities like relict joints and foliations in the subsurface, this kind of slope movement indicates that a rotational-slide type of failure may have been triggered (failure mode 2). The combined failure mode (failure modes 1 and 2) may be described as multiple, translational-slide, and rotational-slide type.

Based on the interpreted field monitoring results, groundwater flow and failure mechanisms are postulated. It will be useful to carry out a comprehensive three-dimensional coupled seepage–stress–deformation analysis to confirm the findings in future.

Acknowledgements

The fieldworks presented in this paper were undertaken as part of the pilot natural hillside assessment and field instrumentation project commissioned by the Government of the Hong Kong Special Administrative Region (SAR). The support by the Geotechnical Engineering Office, the Civil Engineering and Development Department of the Government of the Hong Kong SAR is gratefully acknowledged. The research funds OAP06/07.EG01 and HKUST/9/CRF/09

provided by Arup and the Research Grants Council of the Government of the Hong Kong SAR, respectively, are acknowledged. This paper is published with the permission of the Head of the Geotechnical Engineering Office and the Director of Civil Engineering and Development, the Government of the Hong Kong SAR.

References

ASTM. 2006. Standard practice for classification of soils for engineering purposes (Unified Soil Classification System). ASTM standard D2487. American Society for Testing and Materials, West Conshohocken, Pa.

Bao, C.G., and Ng, C.W.W. 2000. Keynote lecture: some thoughts and studies on the prediction of slope stability in expansive soils. *In* Proceedings of the 1st Asian Conference on Unsaturated Soils, Singapore, 18–19 May 2000. *Edited by* H. Rarhardjo, D.G. Toll, and E.C. Leong, A.A. Balkema, Rotterdam, the Netherlands. pp. 15–31.

BSI. 1990. Methods of test for soils for civil engineering purposes — Part 2: Classification tests. British standard 1377-2. British Standards Institution (BSI), London.

CSI. 2009. Instruction manual for the 229 heat dissipation matric water potential sensor. Revision 5/09. Campbell Scientific, Inc. (CSI), Logan, Utah.

Evans, N.C., and Yu, Y.F. 2001. Regional variation in extreme rainfall values. GEO Report No. 115. Geotechnical Engineering Office (GEO), the Civil Engineering and Development Department of the Government of the Hong Kong SAR, Hong Kong.

Fredlund, D.G., and Rahardjo, H. 1993. Soil mechanics for unsaturated soils. John Wiley and Sons, New York.

Gasmo, J., Hritzuk, K.J., Rahardjo, H., and Leong, E.C. 1999. Instrumentation of an unsaturated residual soil slope. Geotechnical Testing Journal, **22**(2): 128–137.

GCO. 1982. Mid-level studies: report on geology, hydrology and soil properties. Geotechnical Control Office (GCO), Hong Kong.

GEO. 2007. Landslide assessment and monitoring work at four selected sites — feasibility study. Final geological assessment report for Tung Chung Foothills study area. Geotechnical Engineering Office (GEO), the Civil Engineering and Development Department of the Government of the Hong Kong SAR, Hong Kong.

Geokon. 2007*a*. Instruction manual — models 4800, 4810, 4815, 4820 and 4830 vibrating-wire earth pressure cells. Geokon, Inc., Lebanon, N.H.

Geokon. 2007*b*. Instruction manual — model 6150 MEMS in-place inclinometer. Geokon, Inc., Lebanon, N.H.

Lam, C.C., and Leung, Y.K. 1994. Extreme rainfall statistics and design rainstorm profiles at selected locations in Hong Kong. Technical Note No. 86. Royal Observatory, Hong Kong.

Lim, T.T., Rahardjo, H., Chang, M.F., and Fredlund, D.G. 1996. Effect of rainfall on matric suctions in a residual soil slope. Canadian Geotechnical Journal, **33**(4): 618–628. doi:10.1139/cgj-33-4-618.

Ng, C.W.W., Zhan, L.T., Bao, C.G., Fredlund, D.G., and Gong, B.W. 2003. Performance of an unsaturated expansive soil slope subjected to artificial rainfall infiltration. Géotechnique, **53**(2): 143–157. doi:10.1680/geot.2003.53.2.143.

Ng, C.W.W., Wong, H.N., Tse, Y.M., Pappin, J.W, Sun, H.W., and Millis, S.W. 2011. Field study of stress-dependent soil-water characteristic curves and hydraulic conductivity in a saprolitic slope. Géotechnique. In press.

Peterson, P., and Kwong, H. 1981. A design storm profile for Hong Kong. Technical Note No. 58. Royal Observatory, Hong Kong.

Rahardjo, H., Lee, T.T., Leong, E.C., and Rezaur, R.B. 2005. Response of a residual soil slope to rainfall. Canadian Geotechnical Journal, **42**(2): 340–351. doi:10.1139/t04-101.

SMO. 1995. Explanatory notes on geodetic datums in Hong Kong. Survey and Mapping Office (SMO), Lands Department, the Government of the Hong Kong SAR, Hong Kong.

Sun, H.W., Wong, H.N., and Ho, K.K.S. 1998. Analysis of infiltration in unsaturated ground. *In* Slope Engineering in Hong Kong: Proceedings of the Annual Seminar, Hong Kong, 2 May 1997. *Edited by* K.S. Li, J.N. Kay, and K.K.S. Ho. A.A. Balkema, Rotterdam, the Netherlands. pp. 101–109.

Sun, H.W., Ho, K.K.S., Campbell, S.D.G., and Koor, N.P. 2000. The 2 July 1997 Lai Ping Road landslide, Hong Kong — assessment of landslide mechanism. *In* Proceedings of the 8th International Symposium on Landslides, Cardiff, Wales, 26–30 June 2000. *Edited by* E.N. Bromhead, N. Dixon, M.L. Ibsen, and E. Sfakianaki. Thomas Telford, London. Vol. 3, pp. 1423–1430.

Varnes, D.J. 1978. Slope movement types and processes. *In* Landslides, analysis and control. Special Report 176. *Edited by* R.J. Schuster and R.J. Krizek. Transportation Research Board, National Academy of Sciences, Washington, D.C. pp. 11–33.

Zhan, T.L.T., Ng, C.W.W., and Fredlund, D.G. 2007. Field study of rainfall infiltration into a grassed unsaturated expansive soil slope. Canadian Geotechnical Journal, **44**(4): 392–408. doi:10.1139/T07-001.